DOI: 10.13009/EUCASS2025-092
11TH EUROPEAN CONFERENCE FOR AERONAUTICS AND SPACE SCIENCES (EUCASS)

SIMULATION OF MULTI-MATERIAL SOLID ROCKET MOTOR GRAIN

Michael Moroff[1], *Marius Hausmann*[1] *Dr. Helmut Ciezki*[2], *Dr. Philip Pietrek*[1]
[1]*Fraunhofer Institute for Chemical Technology (ICT), Pfinztal, Germany*
[2]*German Aerospace Center (DLR), Hardthausen am Kocher, Germany*
Email-Addresses:
michael.moroff@ict.fraunhofer.de · marius.hausmann@ict.fraunhofer.de ·Helmut.Ciezki@dlr.de ·
philip.pietrek@ict.fraunhofer.de
Corresponding Author: Michael Moroff

Abstract

New developments in additive manufacturing of energetic materials promise the ability to produce Solid Rocket Motors (SRMs) with thrust curves tailored to the mission requirements. In order to design these motors a model was developed to predict the burning of a SRM with a multi-material grain (a grain consisting of several different propellants). This model uses a Coupled-Level-Set-and-Volume-Of-Fluid (CLSVOF)-Approach to simulate the surface regression of the burning propellant and the flow of the gas generated by the combustion of the fuel in the combustion chamber and the flow inside the nozzle. This paper shows the results of simulations for single-material grains (for validation of the model) and multi-material grains. These simulations were done to validate the model and to get an understanding for the behavior of SRMs using multi-material grains. This is necessary to design advanced, complex, multi-material SRMs, which can only be produced with additive manufacturing.

Nomenclature

A_{fuel}	Area of the burning surface
A_{throat}	Area of the nozzle throat
c_p	Specific heat capacity at constant pressure
h	sensible Enthalpy
K	Kinetic energy of the gas
p	Pressure of the gas
p_t	Chamber pressure of the motor
p_{ref}	Reference pressure of the combustion rate, is 1.01325 bar
$\dot{q}_{mass}$	Source term for the mass conservation equation
$\dot{q}_{impulse}$	Source term for the impulse conservation equation
$\dot{q}_{energy}$	Source term for the energy conservation equation
$\dot{q}_{species}$	Source term for the species mass fraction transport equation
$\vec{u}$	Velocity of the gas
R	Gas constant of the gaseous products of the propellant
r_b	Burning rate at reference pressure
T_{burn}	Temperature of the gaseous products of the propellant
V_{burn}	Local burning rate
Y_i	Mass fraction of species i
α	Volume fraction of gas inside a cell
α_ϕ	Factor to reduce the flux through a surface between two cells

Copyright © 2025 by M.Moroff. Published by the EUCASS association with permission.

DOI: 10.13009/EUCASS2025-092

κ	Heat capacity ratio
μ_{eff}	Effective dynamic viscosity of the fluid
ν_{eff}	Effective kinematic viscosity of the fluid
ρ	Density of the gas
ρ_α	Product of gas density and volume fraction gas
ρ_{fuel}	Density of the fuel
Φ	Value of the Signed-Distance-Function

1. Introduction

New additive manufacturing methods for energetic materials allow the production of complex, multi-material Solid Rocket Motors (SRMs). The intention is to produce SRMs with thrust curves tailored to mission requirements. To effectively design these specialised SRMs a suitable model is needed. Two connected processes need to be modelled for this purpose: The first is the surface regression of the burning fuel surface and the second is the flow inside the combustion chamber. These processes are linked by the gases produced at the burning surface and the pressure dependency of the surface regression rate. Previous models for single fuel SRMs used a multi-dimensional model for the surface regression and a zero- or one-dimensional model for the flow in the combustion chamber (see Albarado,[1,2]Cavallini[3] and Kiryushkin.[4] For this model a multi-dimensional approach was chosen for both the surface regression and the flow in the combustion chamber. This is done to properly model the spacial difference of surface regression speed due to layers of different fuels and local pressure difference caused by complex geometries. The model developed is based on the Coupled-Level-Set-and-Volume-of-Fluid (CLSVOF) approach to intrate the Level-Set-Method as a model for the surface regression into a computational fluid dynamic (CFD) solver with the Volume-of-Fluid (VOF) approach. The validation of the solver with experimental data for an end-burner type SRM is shown in this paper together with simulation results for several multi-material SRMs using to different fuel combinations in the motor.

2. CLSVOF-Model for SRMs

The model was implemented into an existing CFD solver of the open source library OpenFOAM. Specifically the compressible, transient solver rhoPIMPLEFoam was used. The modified solver addresses the burning surface with the Level-Set-Method (LSM). A detailed description of the modified solver can be found in Moroff et al.[5]

2.1 Level-Set-Method

The LSM is an implicit model to describe the movements of surfaces using the signed-distance-function (SDF) Φ (see Sethian et al.[6–8]). The value of Φ corresponds to the distance to the closest surface element and the sign of Φ is positive inside the fuel, negative inside the gas and the burning surface Φ is zero. Φ is calculated for every point inside the computational domain. The surface regression is modelled by solving the Level-Set-Equation:

$$\frac{\partial \Phi}{\partial t}\Phi_t - V_{burn}|\frac{\partial \Phi}{\partial x}| = 0 \tag{1}$$

V_{burn} is the local combustion rate of the propellant.

2.2 Implementation of VOF

The VOF approach is used to integrate the LSM into the CFD solver. This is done by replacing the density of the gas ρ in the equations with the product of the density and the volume fraction of the gas inside a cell $\rho_\alpha = \rho * \alpha_{fuel}$. This is done for the three conservation equations of mass, impulse and energy, the transport equation of the different species in the gas mixture and the pressure equation:

Mass conservation equation:

$$\frac{\partial \rho_\alpha}{\partial t} + \nabla(\rho_\alpha \vec{u})_f = \dot{q}_{mass} \tag{2}$$

Momentum conservation equation:

$$\frac{\partial \rho_\alpha \vec{u}}{\partial t} + \nabla((\rho\vec{u})_f * \vec{u}) + \nabla(\rho_\alpha \nu_{eff} \nabla(\vec{u})) + \nabla(\rho_\alpha \nu_{eff}\vec{u}) = -\alpha_\phi \nabla p + \dot{q}_{impulse} \tag{3}$$

DOI: 10.13009/EUCASS2025-092

Energy conservation equation:

$$\frac{\partial \rho_\alpha h}{\partial t} + \nabla((\rho\vec{u})_f * h) + \frac{\partial \alpha\rho K}{\partial t} + \nabla((\rho\vec{u})_f * K) + \alpha * \frac{\partial p}{\partial t} = \dot{q}_{energy} \tag{4}$$

With the kinetic energy $K = u^2/2$.
Species transport equation:

$$\frac{\partial Y_i}{\partial t} + \nabla((\rho\vec{u})_f * Y_i) - \nabla\mu_{eff} Y_i = R(Y_i) + \dot{q}_{species} \tag{5}$$

Pressure equation:

$$\nabla * \frac{\rho_\alpha}{A}\alpha_\phi \nabla p = \frac{\partial \rho_\alpha}{\partial t} + \nabla\frac{\rho H}{A} - \dot{q}_{mass} \tag{6}$$

A and H are gained by writing the momentum conservation equation as:

$$M(\vec{u}) = -\alpha_\phi \nabla p \tag{7}$$

The matrix $M(\vec{u})$ can be written as: $M(\vec{u}) = A\vec{u} - H$. A contains the diagonal and H the off-diagonal contributions of $M(\vec{u})$.

3. Simulations

In the first step, the model is validated by comparing simulation results with experimental data. The case chosen for this purpose is an end-burner type SRM. In the second step several different multi-material motors are simulated using the model.

3.1 Validation of the model with experimental data

The motor chosen for the validation of the model has a diameter of 65 mm in the combustion chamber, a nozzle throat diameter of 5.5 mm, a nozzle end diameter of 17.37 mm and an expansion angle of 15°. The fuel grain has a length of 60 mm and the same diameter as the combustion chamber and is composed out of a ADN-GAP mixture. The properties of the propellant used are shown in table 1.

Table 1: Properties of the propellant and exhaust gases used in the validation case.

	Fuel 1
density $[kg/m^3]$	1602
r_b $[mm/s]$	3.85
n [-]	0.44
T_{burn} $[K]$	3097.8
c_p $[J/kg/K]$	1928.5
κ [-]	1.2183
molar mass $[g/mol]$	24.106

The simulations were done with either a laminar model or a k-ω-SST-turbulence model. A turbulent intensity $I = 0.25$ and turbulence length scale $L_{turb} = 0.001$ m were used for the turbulence boundary conditions of the gas produced by the burning surface. These values were estimated by simulating the burning of the composite propellant for different pressures and then calculating the turbulent properties of the flow.

The computational domain used for the simulation, consists out of three regions (see Fig. 1): The combustion chamber containing the fuel grain, the nozzle and an outflow region. The computational domain represents an axial symmetric slice. Two different boundary conditions are used: A wall boundary condition for the combustion chamber and a pressure of 1 bar and a temperature of 300 K as ambient conditions in the outflow region. The wall either uses a fixed temperature of 300 K or a zero gradient condition. These two temperature boundary conditions are chosen to model a cold combustion chamber model and nozzle (high thermal losses through the wall) and an adiabatic wall (no thermal losses through the wall) to account for potential thermal losses through the combustion chamber wall and nozzle wall. In total four different simulations were run.

DOI: 10.13009/EUCASS2025-092

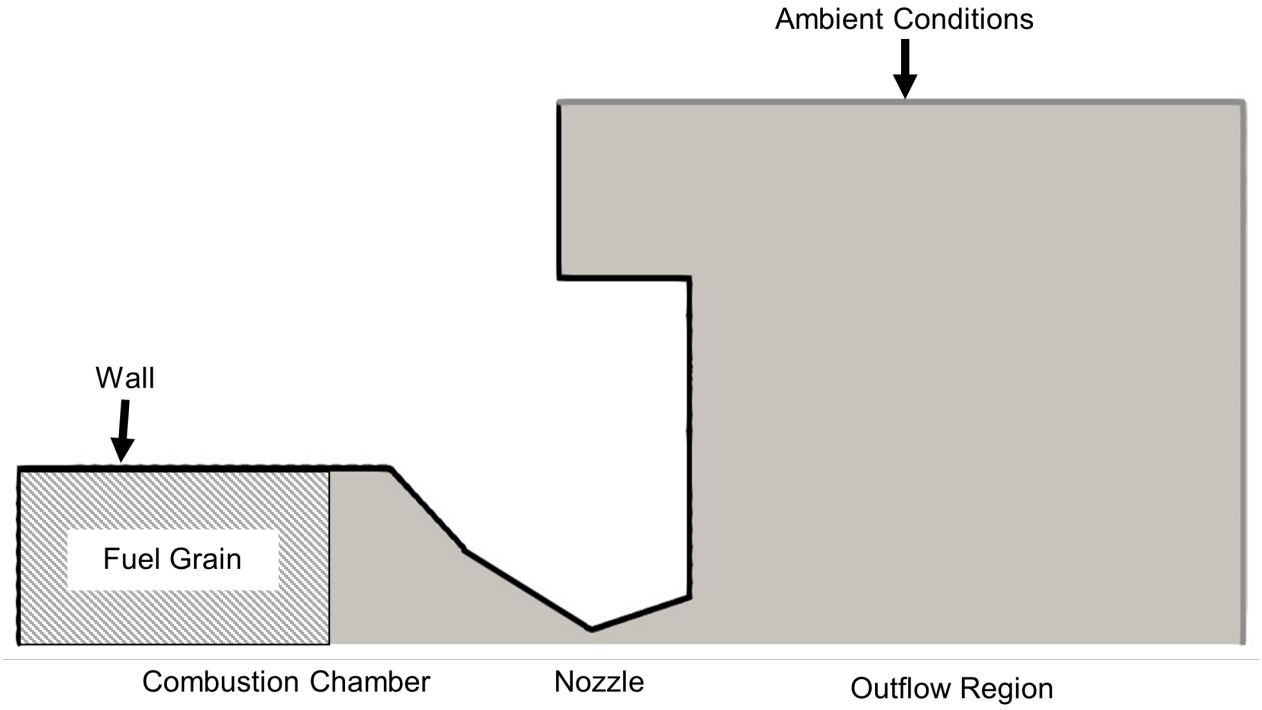

Figure 1: Side view of the computational domain used for the validation simulation. It consists of the combustion chamber (left), the nozzle (middle) and the outflow region (right).

An analytical model was used to compute the chamber pressure p_t during the steady state of the motor firing. The model is based on the assumption that the mass flow into the motor is the same as the mass flow out of the motor. p_t is computed with:

$$p_t = \left(\frac{A_{throat} P_{ref}^n}{A_{fuel} \rho_{fuel} r_b \sqrt{\frac{T_{burn} R}{\kappa}}} \right)^{\frac{1}{n-1}} \tag{8}$$

The resulting thrust and pressure over time for the simulations are shown together with results from an analytical model and experimental data, in figures 2 and for the steady state of the motor in table 2. The thrust at the steady state of the simulations matches the thrust of the experimental data quite well. For the chamber pressure a difference of 13.7% to 14.7% to the experimental data is observed. The comparison between the simulated cases show a small difference in thrust and chamber pressure, which suggest, that the chosen thermal boundary conditions and turbulence model have a very limited impact on thrust (2.0%) and chamber pressure (1.2%). When comparing the experimental data with results from an analytical model, a relatively big difference in thrust together with a very low difference in chamber pressure between experimental data and analytical model is observed. This difference of 13.1% can not be explained by the losses due to the conical nozzle used in the experiment (3.3%). Using the simulated chamber pressure of 88 bar an analytical thrust of 374 N for an ideal nozzle and 362 N for a conical nozzle are calculated. This suggests that losses of 4.7% are caused by viscous flow inside the nozzle and further losses of up to 1.7% of thrust can be attributed to thermal losses. Most of the losses (8.7%) in thrust in the simulation are caused by the loss in total pressure. As for the differences between the chamber pressure of the simulations and the experimental data these might be either explained by some phenomenon in the throat of the nozzle such as a detachment of the flow resulting in a reduced throat area while increasing losses in the nozzle or an inconsistency in pressure measurement in the experiment. To determine the cause of this difference future simulations should use more advanced turbulence models and in some way should model the igniter charge used for the simulations.

DOI: 10.13009/EUCASS2025-092

Table 2: Thrust and pressure of the simulations, the analytical model and the experimental data for the steady state of the SRM.

case	thrust [N]	pressure [bar]
simulation, laminar, adiabatic wall	345.7	89.8
simulation, laminar, fixed wall temperature	342.7	89.0
simulation, turbulent, adiabatic wall	345.9	89.8
simulation, turbulent, fixed wall temperature	339.1	88.7
analytical model	409.9	105.4
experimental data	356.2	104

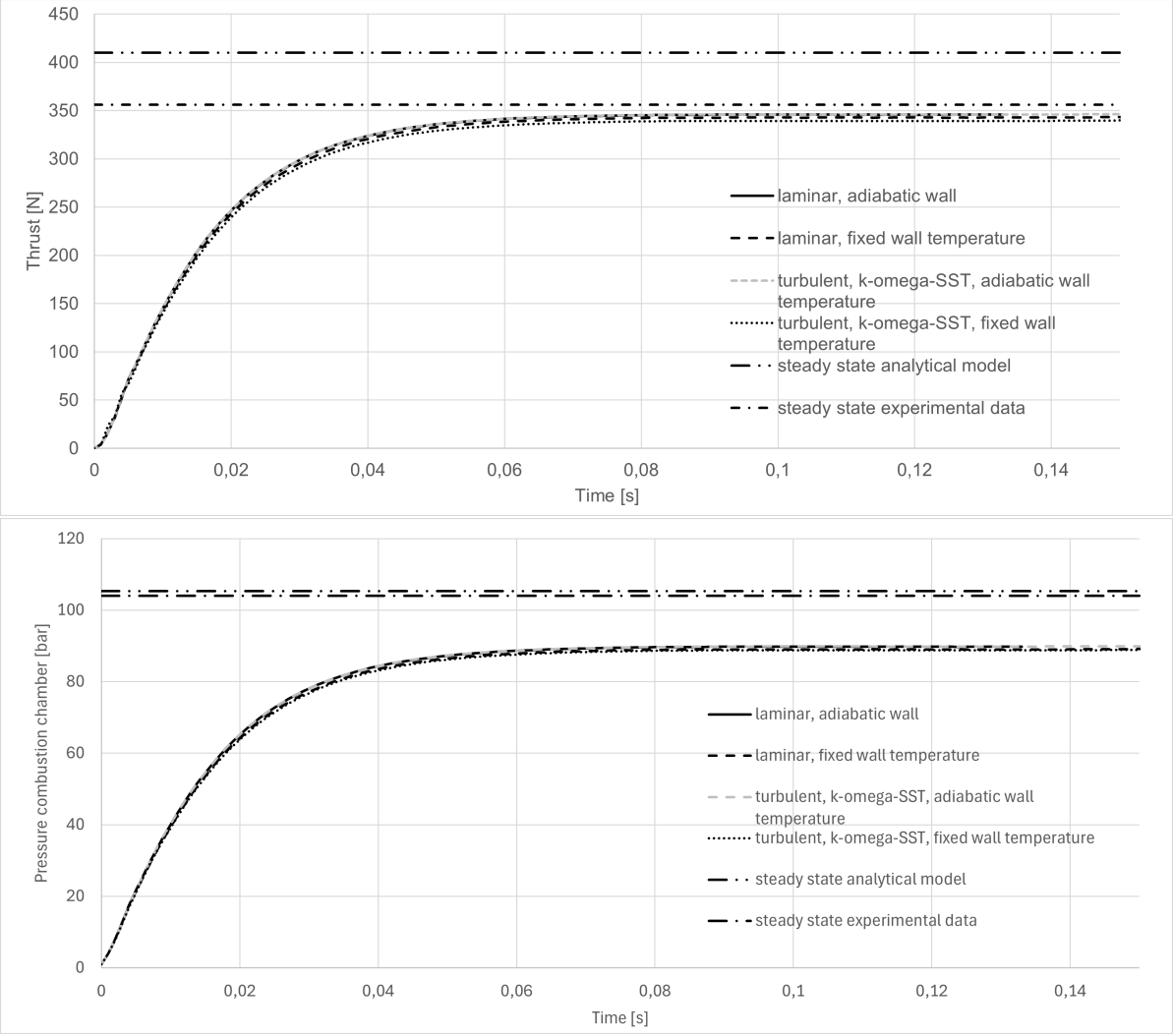

Figure 2: Trust (top) and pressure (bottom) over time for the four simulations, an analytical model and the experimental data for the SRM.

The sum of mass into (produced combustion products) and out (at the end of the nozzle) of the combustion chamber for a simulation are shown in figure 3. The combustion of the fuel grain takes 2.179 s. This matches well with the 2.15 s the fuel needs to burn a distance of 60 mm at a pressure of 89.8 bar.

DOI: 10.13009/EUCASS2025-092

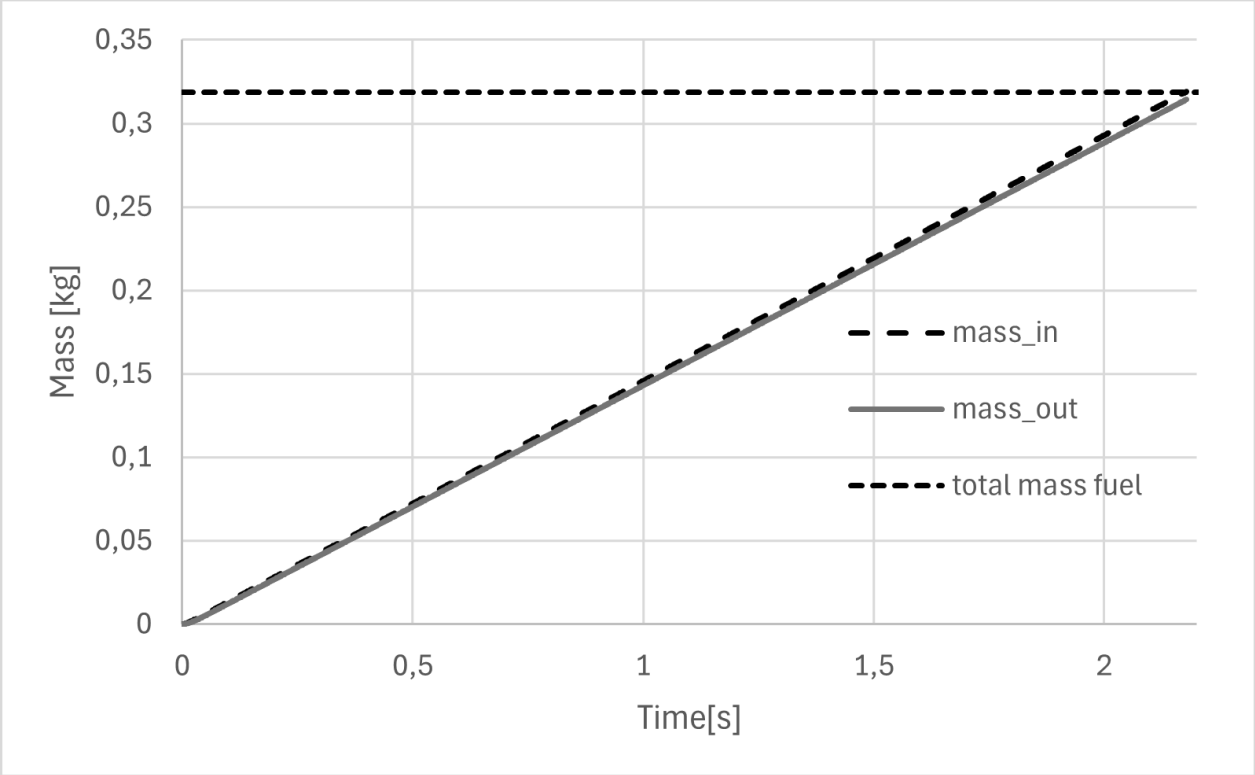

Figure 3: Left: Mass produced at the burning surface (mass_in), mass output through the end of the nozzle (mass_out) and total mass of the fuel grain. The plot is for the simulation with an adiabatic wall and the k-*omega*-SST turbulence model.

Overall the simulations of the SRM show promising results, only the low simulated chamber pressure in comparison to the experiment is an issue. The close match mass_in and mass_out with the mass of the fuel grain, suggests that the difference in chamber pressure is caused by aerodynamic losses in the nozzle. A more advanced turbulence model or a solver based on a central scheme may improve the accuracy of the model with regards to the chamber pressure.

3.2 Simulation of Multi-Material SRMs

To predict the behaviour of multi-material SRMs, a better understanding of the evolution of the burning surface close to the interface between two fuel layers is needed. Two different multi-material geometries were chosen for this purpose, both consist out of a hollow cylinder of one fuel containing a cylinder out of a second fuel. Both cylinder have the same length. The starting surface is set to be the same shape as an end burner. The fuel grain always consists out of a slow burning propellant (refereed to as slow fuel) and one of three fast propellants (fast fuel 1 to fast fuel 3) (see table 3), all four propellants are based on ADN-GAP-propellants.

Table 3: Properties of the different propellants and exhaust gases used for the multi-material simulations

	slow fuel	fast fuel 1	fast fuel 2	fast fuel 3
density $[kg/m^3]$	1596	1683	1632	1602
r_b $[mm/s]$	2.906	2.764	6.154	3.85
n [-]	0.427	0.548	0.474	0.44
T_{burn} $[T]$	2644.1	3084	2983.6	3097.8
c_p $[J/kg/K]$	1929.8	1912.3	1935	1928.5
κ	1.2113	1.2004	1.2146	1.2183
molar mass $[g/mol]$	22.053	24.611	22.82	24.106

The diameter of the hollow and inner cylinder are chosen so the burning surface of the fast fuel is one third the area of the slow fuel. The fuel grains where the inner cylinder consists out of the slow fuel and the hollow outer

DOI: 10.13009/EUCASS2025-092

cylinder consists out of fast fuel are referred to as "slowInside" and fuel grains where the inner cylinder consists out of the fast fuel and the hollow outer cylinder consists out of slow fuel are refereed to as "fastInside" (see Fig 4). The combustion chamber of the motor has a diameter of 65 mm and the nozzle has a throat diameter of 7.5 mm.

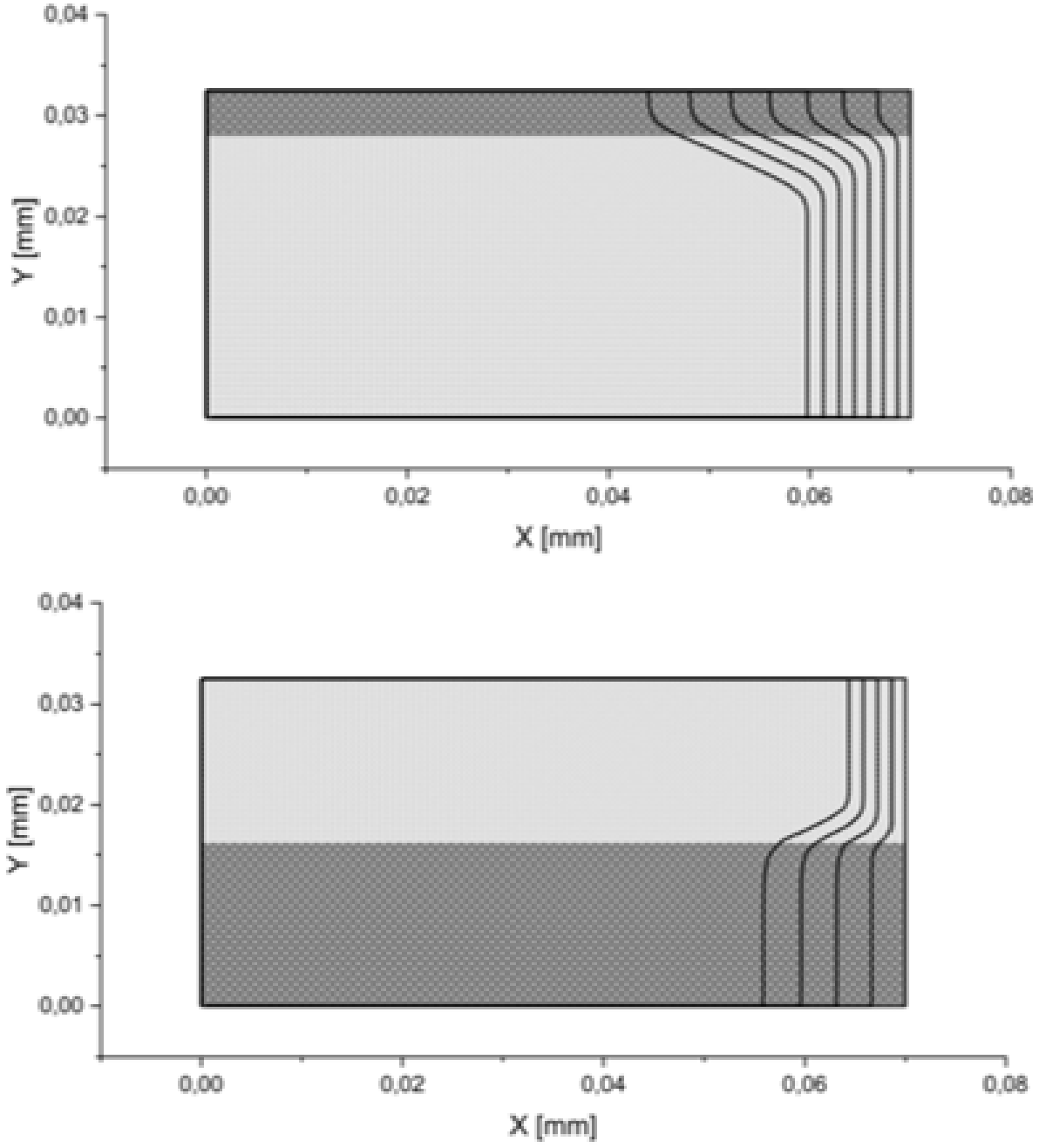

Figure 4: Top: Surface regression for a motor with the fast fuel on the inside and the slow fuel on the outside. Bottom: Surface regression for a motor with the fast fuel on the outside and the slow fuel on the inside. The fuels used are slow fuel (light gray) and fast fuel 2 (dark gray), the propellants burn from left to right. The time difference between each line is 100 ms.

The burning surface inside the slow fuel develops a diagonal transition between the two fuel layers (see Fig 4). The resulting gradient of the burning surface depends on the ratio of the combustion rates of the two fuels. The larger the difference in combustion rates of the two fuel is, the steeper the angle of the burning surface close to the fuel layer interface is. The gradient β of the diagonal transition of the burning fuel surface between the fuel layers can be approximated with (see table 4 and Fig 5):

DOI: 10.13009/EUCASS2025-092

$$\beta = \frac{V_{slowfuel}}{V_{fastfuel}} \tag{9}$$

Table 4: β for the six simulation cases. The camber pressure of the simulation was used to calculate the combustion velocities for β.

	fast fuel 1	fast fuel 2	fast fuel 3
β	0.70	0.39	0.72

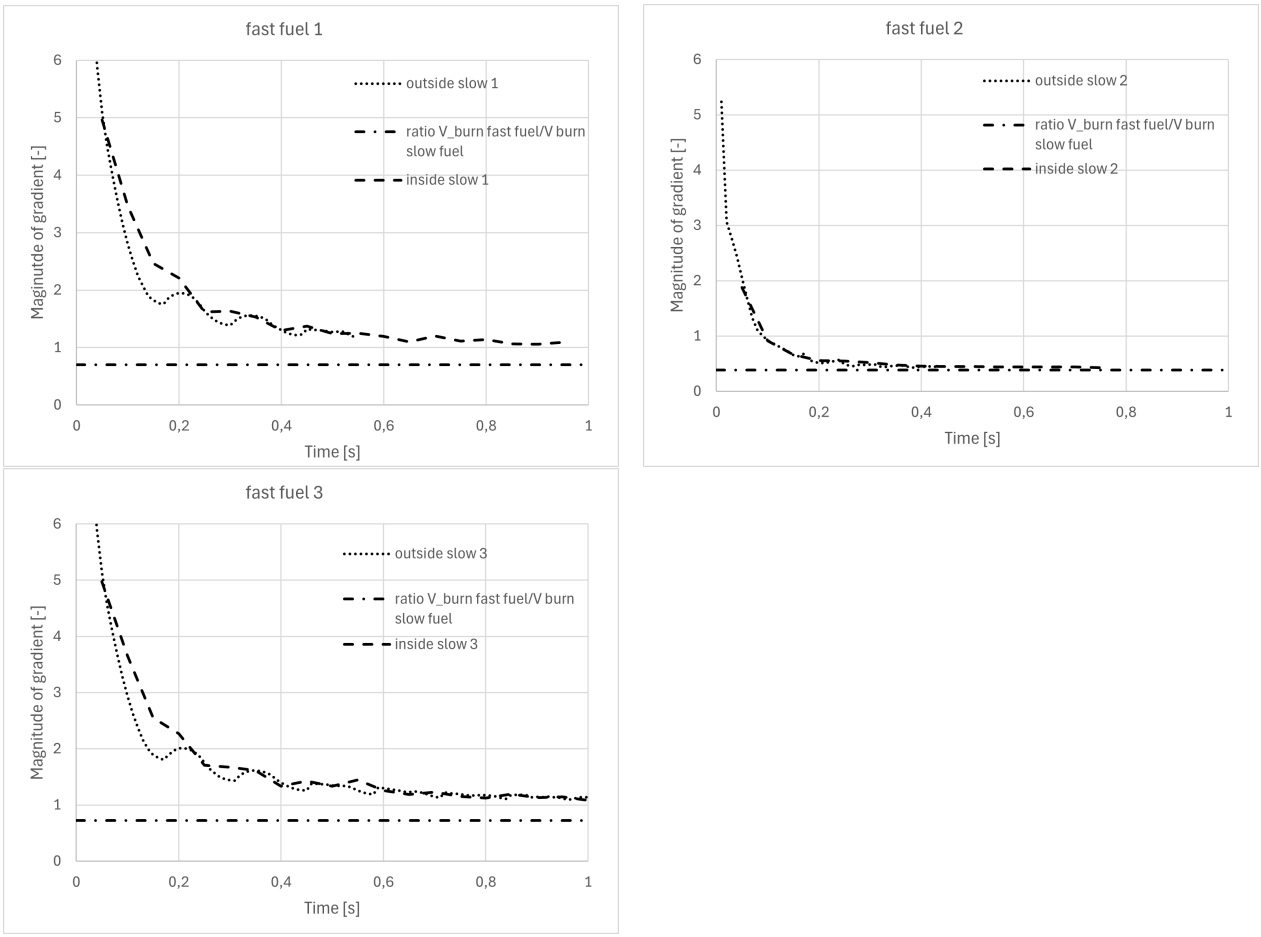

Figure 5: Gradient of the burning surface close to the fuel layer interface. The fuels used are slow fuel and fast fuel 1.

4. Conclusion

The solver presented and investigated here was developed to simulate multi-material SRMs. To validate the model four different simulation results were compared with analytical results and experimental data. The steady thrust of the simulations show a good match with the experimental data. The chamber pressure shows a bigger difference, the cause for this behaviour is not yet fully clear and will be investigated in the future. The choice of turbulence model and thermal boundary condition show a very limited influence on thrust and pressure so far.

The solver was also used to investigate the combustion behaviour of multi-material SRMs. Six different multi-material test cases were simulated. From the results a direct connection between the angle between the burning surface and the fuel layer interface and the combustion velocity's of the fuels could be observed. This connection will prove useful when designing multi-material SRMs in the future. Overall the validation of the CLSVOF-solver has shown great results an the potential for the design of new multi-mission SRMs.

DOI: 10.13009/EUCASS2025-092

References

[1] Kevin Albarado, Andrew Shelton, and Roy J. Hartfield. Srm simulation using the level set method and higher order integration schemes, 30.7-1.8.2012.

[2] Kevin M. Albarado. *Application of the Level Set Method to Solid Rocket Motor Simulation*. Masterarbeit, Auburn University, Auburn, Alabama, 4.8.2012.

[3] Enrico Cavallini. *Modeling and Numerical Simulation of Solid Rocket Motors Internal Ballistics*. Dissertation, Sapienza University of Rome, Rom, 2009.

[4] A. E. Kiryushkin and L. L. Minkov. Solution of internal ballistic problem for srm with grain of complex shape during main firing phase. *Journal of Physics: Conference Series*, 894:012041, 2017.

[5] Michel Moroff, Philip Pietrek, Helmut Ciezki, Stefan Schlechtriem. Coupled-level-set-and-volume-of-fluid (clsvof)-model for the simulation of heterogeneous solid rocket motors. *Proceedings of the 9th EDITION OF THE 3AF INTERNATIONAL CONFERENCE ON SPACE PROPULSION*, 2024.

[6] J. A. Sethian. A fast marching level set method for monotonically advancing fronts. *Proceedings of the National Academy of Sciences*, 93, 1996.

[7] J. A. Sethian. Advances in fast marching and level set methods for propagationg interfaces. *Internationl Series of Numerical Mathematics*, 130(855-864), 1999.

[8] J. A. Sethian. Evolution, implementation, and application of level set and fast marching methods for advancing fronts. *Journal of Computational Physics*, 169(169):503–555, 2001.